Dynamics of Au-Ge liquid droplets on Ge(1 1 1) terraces: Nucleation, growth and dynamic coalescence

Ali El-Barraj, Stefano Curiotto, Fabien Cheynis, Pierre Müller, Frédéric Leroy

Preprint published in Applied Surface Science 509 (2020) 144667
https://doi.org/10.1016/j.apsusc.2019.144667

Dynamics of Au-Ge liquid droplets on Ge(111) terraces: nucleation, growth and dynamic coalescence

Ali El-Barraj[a], Stefano Curiotto[a], Fabien Cheynis[a], Pierre Müller[a], Frédéric Leroy[a,*]

[a] *Aix Marseille Univ, CNRS, CINAM, Marseille, France*

Abstract

Nucleation, growth and coalescence of 3D Au-Ge droplets on Ge(111) surface have been studied in real time by Low Energy Electron Microscopy. Based on the dependence of the droplets surface density with temperature and Au deposition rate, the surface diffusion energy barrier of Au on Ge(111) is estimated as 1.5 ± 0.2 eV. At long time scale it is also shown that the droplets have a brownian motion that results in dynamic coalescence events. From the decrease of the droplet number, the size dependence of the diffusion coefficient of the droplets is shown to decay as $R^{-1.9\pm0.5}$ where R is the droplet radius. This result indicates that the spontaneous motion of the droplets is controlled by an interfacial mass transport phenomenon.

1. Introduction

Semiconducting nanowires are very attractive [1] for future applications in nanoelectronics [2–4] or optoelectronics [5, 6]. Their fabrication is mainly based on a bottom-up approach [7] using the Vapor-Liquid-Solid (VLS) mechanism [8–10] in which a metal-semiconductor liquid alloy is acting as intermediate in the growth process. Surface and interface phenomena occurring between these alloys and the substrate are crucial in the perspective of controlling the growth. For instance under specific conditions either vertical [11, 12] or lateral [13, 14] Si nanowires catalyzed by Au-Si nanodroplets can be grown *via* the VLS mechanism. In these processes surface diffusion phenomenon and the ability of the droplets to incorporate metal atoms or etch the semiconductor surface are crucial. These processes are exacerbated by the large surface to volume ratio of the nanometer size droplets and are intimately related to the energetics of the nanoalloys and the kinetics of mass transfers at the interface with the substrate. For instance in the case of Si nanowires catalyzed by Au-Si droplets, the surface diffusion of Au on Si has been studied as well as the Au-Si alloys droplets formation and kinetics [15–19]. In particular it has been shown that Au-Si droplets on Si(111) during Au deposition spontaneously move in the direction of upward steps to dissolve Si and reach the liquidus composition [20]. This behaviour differs from Au-Si droplets on Si(100) that are not mobile and etch locally the Si substrate. It also differs from Au-Si droplets on Si(110) that move and etch the substrate along the $\langle 110 \rangle$ crystallographic axis [14]. These striking differences highlight the role of the surface orientation on mass transfer kinetics and show that interfacial processes can be dominant in particular on densely packed surfaces such as Si(111). In the case of Ge nanowires catalyzed by Au-Ge alloy droplets, despite numerous studies of the vertical nanowires growth on Ge(111) [21–28] and structural/morphological studies [29–31], nucleation, growth and migration dynamics of Au-Ge droplets on Ge(111) surface have still to be addressed. In this article we aim at describing the nucleation, growth and coalescence of Au-Ge droplets close to the eutectic temperature. Based on the measurement of the Au-Ge droplets density on Ge(111) surface as function of Au deposition flux and temperature we show that the critical nucleus is made of 2 atoms and the surface diffusion energy barrier of Au on Ge(111) is 1.5 ± 0.2 eV. The growth process of the droplets on terraces is dominated by a dynamic coalescence mechanism induced by the spontaneous motion of the droplets at the surface.

2. Experimental details

The experiments were performed in an Ultra High Vacuum (UHV) setup equipped with a Low Energy Electron Microscope (LEEM) [32]. Ge(111) substrates were cut into samples of 9×9 mm^2, cleaned under ultrasonic bath with acetone, ethanol and distilled water, and mounted onto the LEEM sample holder before introduction in the UHV. The LEEM sample holder has an integrated tungsten filament to heat the sample by radiation and electron bombardment. The Ge(111) surface was cleaned by repeated Ar^+ ion bombardment at 1 keV (current: 10 μA) and annealing close to the melting point of Ge in a dedicated UHV

*Corresponding author
Email addresses: elbarraj@cinam.univ-mrs.fr (Ali El-Barraj), curiotto@cinam.univ-mrs.fr (Stefano Curiotto), cheynis@cinam.univ-mrs.fr (Fabien Cheynis), muller@cinam.univ-mrs.fr (Pierre Müller), leroy@cinam.univ-mrs.fr (Frédéric Leroy)

preparation chamber. Au was dosed from a Knudsen evaporator (MBE Komponenten) at a typical deposition rate of 0.1 ML per minute. Au was deposited during LEEM imaging, so that growth and motion phenomena could be directly observed with a typical lateral resolution of 10 nm. The LEEM image sequences were taken with a typical frequency of 1 Hz. The Au deposition rate was calibrated for different temperatures of the Au source (1423 K to 1498 K) by assuming the saturation coverage of the Ge(111)-$\sqrt{3}\times\sqrt{3}$-Au reconstructed surface in this temperature range to be 1 ML [33]. The surface evolution and growth were studied in bright field mode, with an electron beam energy of 3 eV. The sample temperature was measured with a thermocouple positioned under an edge of the sample and using an optical pyrometer with the emissivity of Ge [34] (0.55). The thermocouple calibration was corrected assuming that the phase transition temperature of the 1×1 to $\sqrt{3}\times\sqrt{3}$ R30° occurs at 913 K for a complete ML of Au at the surface [33].

3. Results and discussion

The growth of Au on Ge(111) was studied from 580 K up to 700 K. After completion of the first atomic layer of Au, the substrate exhibits a Ge(111)-$\sqrt{3}\times\sqrt{3}$-Au reconstructed surface. Going on with Au deposition, fuzzy and highly mobile bright structures appear in LEEM (see fig. 1a) and then form dark particles that nucleate preferentially at step edges but also in the middle of extended terraces ($> 1\mu$m). As shown by Hajjar [29] the initial occurrence of bright structures could be assigned to the formation of 2D metastable islands of Au. These islands are highly mobile at the Ge(111) surface and after a lag time they spontaneously form 3D Au-Ge liquid droplets (black contrast) as expected from the deep Au-Ge eutectic in the bulk phase diagram ($Au_{72}Ge_{28}$ (633 K) [35]). For temperatures lower than the bulk eutectic temperature, small liquid droplets still form at the surface due to the decrease of the eutectic temperature for nanometer size alloys as shown for Au-Ge [24, 36] or Au-Si alloys [37, 38].

To study mass transport mechanisms at the surface we have first observed the evolution of the droplets surface density (number of droplets per unit surface) as a function of temperature. The inset of figure 1b shows two LEEM images obtained at 661 and 693 K. In this measurements Au was deposited at 1.05×10^{16} m^{-2} s^{-1} ($\sim$ 0.1 ML.min^{-1}). The density of Au droplets has been estimated only on atomically extended flat terraces (area $\sim$20 μm^2) and at the maximum density before coalescence occurs. This droplet density is strongly temperature dependent. Figure 1b shows an Arrhenius plot of the droplet density. The droplet density decrease with temperature is related to the Au adatom diffusion coefficient. At high temperature Au adatoms can diffuse over much longer distances than at low temperature before forming a stable nucleus. As a consequence, droplets formed at high temperatures are less numerous but larger than those formed at low temperatures.

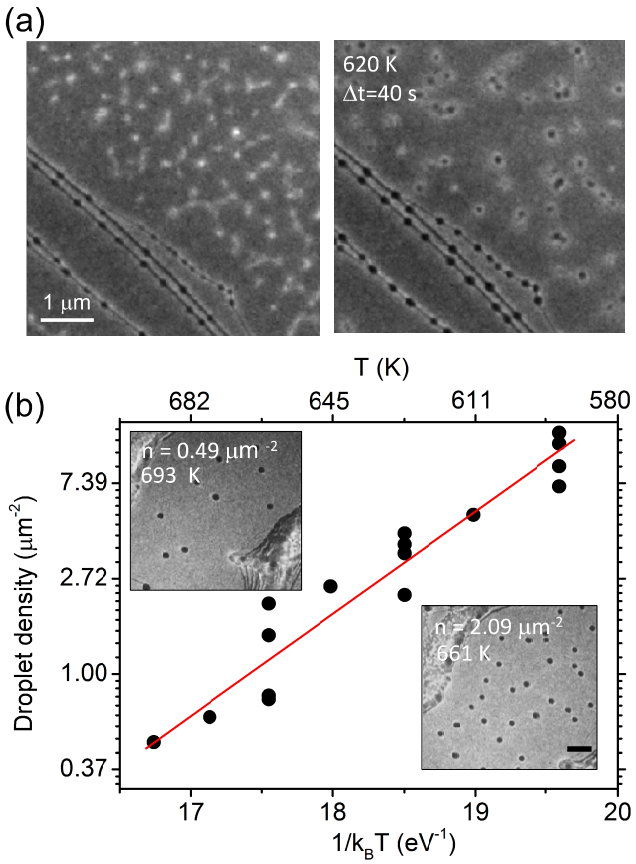

Figure 1: (a) Bright field images (E=3 eV) during growth of Au on Ge(111)-$\sqrt{3}\times\sqrt{3}$-Au: Au bright and fuzzy structures nucleate first and then droplets occurs (appearing as black circles). Scale bar: 1 μm. (b) Plot and fit of the droplets density as function of $(k_BT)^{-1}$. The dispersion of data points illustrates the error bars. Inset LEEM images at two temperatures before coalescence.

The nucleation and growth at surfaces have been extensively described in the framework of the theory proposed by Venables et al. [39]. This approach is based on a kinetic description of diffusion and condensation processes of adatoms. It has been shown that the droplets density [39] N can be written in the following way:

$$\ln(N) = \ln(\eta(Z)\cdot N_0) + p\ln\left(\frac{1}{N_0\upsilon}\right) + p\ln(R) + \frac{E}{k_BT} \quad (1)$$

where Z is the surface coverage, $\eta(Z)$ is a coverage dependent parameter, υ is an effective surface vibrational frequency (physical range 10^{11} to 10^{13} Hz). R is the deposition rate and N_0 is the density of atomic sites at the surface ($7.22\,10^{18}$ m^{-2}). The effective energy E is given by $E = \frac{E_i + iE_d}{i+2}$ in the regime of 2D nucleation and complete condensation. i is the critical number of atoms in a cluster to be stable and $p = \frac{i}{i+2}$. E_i is the binding energy of a cluster of i atoms and E_d is the energy barrier for atoms

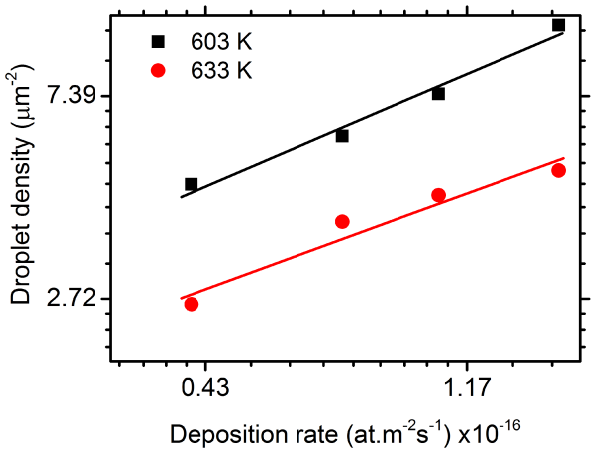

Figure 2: Plot and fit of the droplets density as function of Au deposition rate at $T = 603$ K and $T = 633$ K.

diffusion at the surface. From eq. 1, the linear fit of $\ln(N)$ as a function of $(k_B\mathrm{T})^{-1}$ where k_B is the Boltzmann's constant and T the temperature (see figure 1b) provides the effective energy E. The slope of the linear fit of the data gives $E = 1.07 \pm 0.06$ eV [40]. In order to obtain a precise estimate of the critical nucleus size i, we have also studied in a second set of experiments the droplets density (before coalescence) as a function of the Au deposition rate (R) and at different temperatures (see figure 2). From eq. 1, as $\ln(N) \sim p\ln(R)$, we obtain $p = 0.51 \pm 0.06$ and thus the critical nucleus size is $i = -\frac{2p}{p-1} = 2.04 \pm 0.15 \sim 2$ atoms. If a third atom joins the critical nucleus, the cluster becomes stable as expected for a threefold symmetry surface. This small value for the critical nucleus size validates *a posteriori* the hypothesis of 2D nucleation.

From the effective energy E and the critical nucleus size i we can estimate the diffusion energy E_d of Au atoms on Ge(111)-$\sqrt{3}\times\sqrt{3}$-Au reconstructed surface. We assume that the cluster cohesion energy is just the strength of Au-Au bonds in a cluster of i Au atoms. From the heat of sublimation of Au (3.83 eV/atom), the binding energy per atom is estimated equal to $3.83/6 = 0.64$ eV. Thus we find that $E_d = \frac{E(i+2)-E_i}{i} = 1.5 \pm 0.2$ eV. This value is comparable but higher than that found for the diffusion of Au on Si (1.3 ± 0.2 eV [16]), a system analogous to Au-Ge.

After the droplets formation stage it appears that the droplets are mobile on terraces and are pinned at step edges (see Fig. 3-(a)-(c)) or domain boundaries of the $\sqrt{3} \times \sqrt{3}$ surface reconstruction [40]. This behaviour is different from that of Au-Si droplets that are immobile on terraces without Au deposition [20]. Figures 3(b) shows the projection of 150 images (Δt=315 s) of Au-Ge droplets diffusing by brownian motion on the surface. The LEEM movies clearly show that the number of droplets decays by coalescence events taking place during their brownian motion (dotted circles in Figures 3(a) show areas where two droplets have coalesced). Thus contrary to the conventional hypothesis of Ostwald ripening [29] to explain

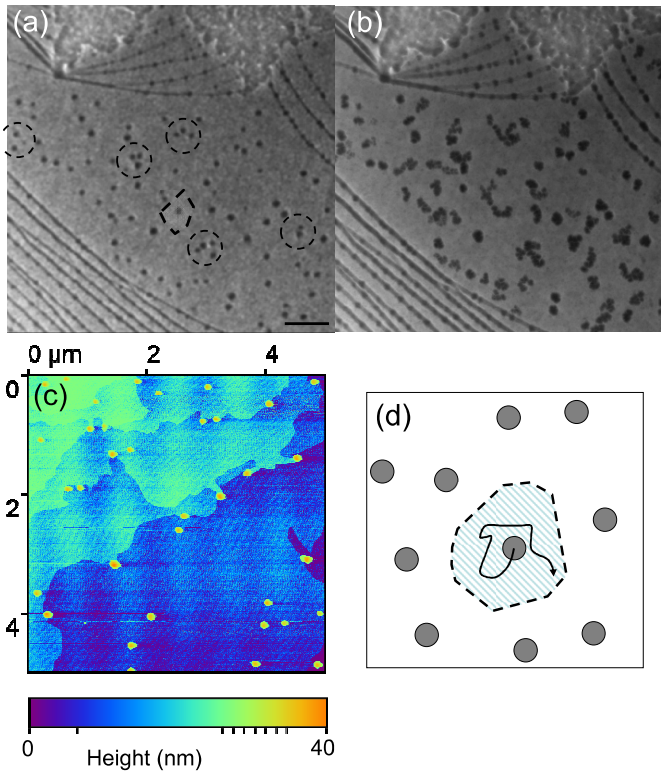

Figure 3: (a) Bright field LEEM image of Au droplets during coalescence at 604 K (Scale bar: 1 μm.). See Supplemental Material at [URL will be inserted by publisher] for the complete movie. Doted circles: coalescence of 2 droplets (within 100 s). Dotted line: a Voronoï cell is schematically drawn around one droplet. (b) Projection of 150 images (over 315 s) showing the spontaneous motion of the droplets on the terrace. (c) AFM image topography of the surface after quenching (field of view 5× 5 μm^2). 3D droplets are pinned at step edges but are also visible on extended terraces (> μm^2). (d) Schematic description of the dynamic coalescence process and Voronoï cell.

the decay of droplets density upon annealing, LEEM real time measurements enable to show without any ambiguity that the decay originates from a dynamic coalescence process. Additionally we observe no significant change of the droplet size during their migration. Based on simulations and analytical approaches, Meakin [41] has developed a general theory to describe the time evolution of the number of droplets at a surface when the leading mechanism for growth is the dynamic coalescence between mobile droplets. Very importantly it is shown that the decay rate of the droplets number is related to the size dependence of the droplet diffusion coefficient. The decay of droplets number N on a surface area S by coalescence during time dt can be written as: $dN \propto -N\frac{dt}{\tau}$ where τ is the time for a collision to occur between two neighboring droplets. τ can be estimated as the time for a droplet to explore by a random motion its Voronoï cell area (Fig. 3(d)). As the mean Voronoï cell area is S/N, thus $\tau = \frac{S}{ND(R)}$ and then $dN \propto -N^2D(R)/Sdt$. The N^2 dependence of the decay rate of droplets number is related to a mechanism of dynamic coalescence of two droplets which is the dominant

mechanism with respect to higher order processes involving simultaneous coalescence of 3 and more droplets. Assuming now global mass conservation and a scaling law[42] for $D(R) \propto R^{-\alpha}$, where R is the droplet radius and α is an exponent, we can calculate explicitly the time evolution of the droplets number at the surface. The value of the α exponent contains key information on the atomic mechanisms controlling the mass transport responsible for the diffusion of the droplets [42]. For 3D structures it has been established that α=2 corresponds to a limiting mechanism of attachment and detachment of atoms; α=3 to a mechanism of volume diffusion of atoms and α=4 to a mechanism of diffusion of atoms at the interface. Considering an additional logarithmic correction due to the two-dimensional random walk [41], the time evolution of the number of droplets in the asymptotic regime reads:

$$N(t) \approx (\frac{t}{\ln(t)})^{-\frac{3}{3+\alpha}} \quad (2)$$

The experimental natural logarithm of the normalized number of droplets as function of $\ln(\frac{t}{\ln(t)})$ is reported in figure 4 for different temperatures. The slope of the asymptotic fit of the droplets number gives the exponent $\frac{3}{3+\alpha} = 0.61 \pm 0.10$ and we deduce an estimate of $\alpha = 1.9 \pm 0.5$. The high value of α suggests that, among the three motion mechanisms considered above, a brownian motion limited by interfacial attachment-detachment (called also evaporation-condensation) of atoms at the droplet/substrate interface is the most adequate. However from the uncertainty on the α value we cannot exclude that even slower processes of mass transport occur. For instance, considering that the dissolution of the Ge substrate in the Au-Ge droplets may induce the formation of a hole under the droplet [14, 29] and the development of a faceted interface, mass transport may be hindered by nucleation mechanisms of atomic layers at the interface [43, 44]. These nucleation mechanisms may be required to dissolve (resp. crystallize) the substrate at the front (resp. back) side of the moving droplet. This type of behaviour may lead to a fast decay of the diffusion coefficient with respect to the droplet size. Let us note that droplet migration of metal-semiconductor alloys have also been studied in the presence of a driving force such as an electric current or an applied thermal gradient as observed in Au/Ge(110)[45], Pt/Si(001)[46], Au/Si(100)[47] or Pt/Ge(110)[48] systems. The directed motion of the liquid eutectic droplets is due to the concentration gradient induced by the external applied force. In these studies it has been proposed that the limiting kinetic mechanism for atomic transport is volume diffusion across the droplet whereas we find that attachment-detachment kinetics of atoms at the droplet-substrate interface could be the limiting mechanism for Au-Ge droplets on Ge(111). To understand these differences in the proposed mechanism we can note that the studies are performed in different regimes: the Au-Ge droplets studied here have a size in the range 50-100 nm and randomly move on flat terraces at a temperature close to the eutectic temperature. In the previously mentioned studies, droplets are micrometric, the temperature range is well above the eutectic temperature (900 K) and the droplets pass across steps suggesting that the surface properties play a minor role in the mechanism. Therefore we infer that the droplets behave differently in both cases and that size dependent measurements of the velocity could help to distinguish the underlying atomic processes.

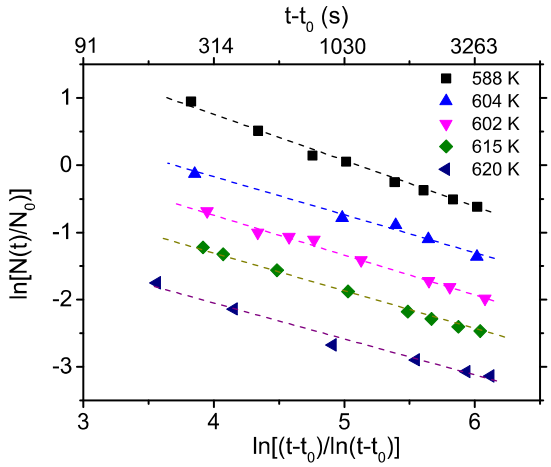

Figure 4: Ln of the normalized evolution of the number of droplets as function of $ln[(t-t_0)/ln(t-t_0)]$ for different temperatures. For clarity the data are offset vertically. The dashed lines show the asymptotic fit of the data.

4. Conclusions

We have studied *in situ* the nucleation, growth and coalescence of Au droplets on Ge(111) by LEEM. From temperature and flux dependencies of the droplet number per surface unit we have found that the surface diffusion energy of Au on Ge(111) is 1.5 ± 0.2 eV and the critical nucleus size is made of 2 atoms. Continuing the investigations after deposition, we have observed that the droplets spontaneously move on the substrate and grow by dynamic coalescence, while Ostwald ripening plays only a minor role. From a study of the coalescence dynamics, we show that the droplet motion is mainly limited by attachment-detachment of atoms at the droplet/substrate interface.

Acknowledgments

We acknowledge the financial support of the ANR grant HOLOLEEM (ANR-15-CE09-0012). We thank the CINaM-Planete facility and A. Ranguis for the technical support. We are grateful to B. Ranguelov and M. Michailov for stimulating discussions we had in the framework of the PHC Rila project (38663TB).

Declarations of interest: none

References

References

[1] J. Hu, T. Odom, C. Lieber, Accounts of Chemical Research 32 (5) (1999) 435–445.

[2] Y. Huang, X. Duan, Q. Wei, C. Lieber, Science 291 (5504) (2001) 630–633.

[3] M. Gholipour, N. Masoumi, Microelectronics Journal 44 (3) (2013) 190–200.

[4] Y. Cui, C. Lieber, Science 291 (5505) (2001) 851–853.

[5] W. Guo, M. Zhang, A. Banerjee, P. Bhattacharya, Nano Letters 10 (9) (2010) 3355–3359.

[6] S. M. Sadaf, S. Zhao, Y. Wu, Y. H. Ra, X. Liu, S. Vanka, Z. Mi, Nano Letters 17 (2) (2017) 1212–1218.

[7] L. Guniat, P. Caroff, A. F. i Morral, Chemical Reviews 119 (15, SI) (2019) 8958–8971.

[8] R. S. Wagner, W. C. Ellis, Applied Physics Letters 4 (1964) 89–90.

[9] R. S. Wagner, W. C. Ellis, Transactions of the Metallurgical Society of AIME 233 (1965) 1053–1063.

[10] T. I. Kamins, X. Li, R. Stanley Williams, X. Liu, Nano Letters 4 (2004) 503–506.

[11] F. M. Ross, J. Tersoff, M. C. Reuter, Physical Review Letters 95 (14) (2005) 146104.

[12] S. Kodambaka, J. Tersoff, M. C. Reuter, F. M. Ross, Physical Review Letters 96 (9) (2006) 096105.

[13] S. Curiotto, F. Leroy, F. Cheynis, P. Müller, Nano Letters 15 (2015) 4788.

[14] S. Curiotto, F. Leroy, F. Cheynis, P. Müller, Scientific Reports 7 (2017) 902.

[15] W. Swiech, E. Bauer, M. Mundschau, Surface Science 253 (1991) 283–296.

[16] S. Curiotto, F. Cheynis, F. Leroy, P. Müller, Surface Science 647 (2016) L8–L11.

[17] M. I. Den Hertog, J.-L. Rouviere, F. Dhalluin, P. J. Desré, P. Gentile, P. Ferret, F. Oehler, T. Baron, Nano Letters 8 (2008) 1544–1550.

[18] F. Ruffino, A. Canino, M. G. Grimaldi, F. Giannazzo, F. Roccaforte, V. Raineri, Journal of Applied Physics 104 (2) (2008) 024310.

[19] N. Ferralis, F. El Gabaly, A. K. Schmid, R. Maboudian, C. Carraro, Physical Review Letters 103 (2009) 256102.

[20] S. Curiotto, F. Leroy, F. Cheynis, P. Müller, Surface Science 632 (2015) 1–8.

[21] H. Adhikari, A. F. Marshall, I. A. Goldthorpe, C. E. D. Chidsey, P. C. McIntyre, ACS Nano 1 (5) (2007) 415–422.

[22] A. D. Gamalski, J. Tersoff, R. Sharma, C. Ducati, S. Hofmann, Nano Letters 10 (8) (2010) 2972–2976.

[23] S. Kodambaka, J. Tersoff, M. C. Reuter, F. M. Ross, Science 316 (5825) (2007) 729–732.

[24] E. A. Sutter, P. W. Sutter, ACS Nano 4 (8) (2010) 4943–4947.

[25] E. A. Sutter, P. W. Sutter, Nanotechnology 22 (29) (2011) 295605.

[26] P. W. Sutter, E. A. Sutter, Nature Materials 6 (5) (2007) 363–366.

[27] A. Sundar, P. Farzinpour, K. D. Gilroy, T. Tan, R. A. Hughes, S. Neretina, Small 10 (16) (2014) 3379–3388.

[28] B. J. Kim, C. Y. Wen, J. Tersoff, M. C. Reuter, E. A. Stach, F. M. Ross, Nano Letters 12 (11) (2012) 5867–5872.

[29] S. Hajjar, G. Garreau, L. Josien, J. L. Bubendorff, D. Berling, A. Mehdaoui, C. Pirri, T. Maroutian, C. Renard, D. Bouchier, M. Petit, A. Spiesser, M. T. Dau, L. Michez, V. L. Thanh, T. O. Mentes, M. A. Nino, A. Locatelli, Physical Review B 84 (12) (2011) 125325.

[30] H. Zitouni, A. Mehdaoui, A. Spiesser, K. D. Khodja, L. Josien, V. Le Thanh, C. Pirri, Acta. Mat. 90 (2015) 310–317.

[31] A. P. Kryshtal, A. A. Minenkov, P. J. Ferreira, Interfacial kinetics in nanosized Au/Ge films: An in situ TEM study, Applied Surface Science 409 (2017) 343–349.

[32] F. Cheynis, F. Leroy, A. Ranguis, B. Detailleur, P. Bindzi, C. Veit, W. Bon, P. Müller, Review of Scientific Instruments 85 (2014) 043705.

[33] G. Le Lay, Surface Science 132 (1983) 169–204.

[34] F. G. Allen, Journal of Applyed Physics 28 (1957) 1510.

[35] P. Y. Chevalier, Thermochimica Acta 141 (1989) 217–226.

[36] H. Lu, X. Meng, Sci. Rep. 5 (2015) 11263.

[37] S. Bajaj, M. G. Haverty, R. Arroyave, W. A. Goddard, S. Shankar, Nanoscale 7 (2015) 9868.

[38] T. Tanaka, S. Hara, Zeitschrift für Metallkunde 92 (2001) 467.

[39] J. A. Venables, G. D. T. Spiller, M. Hanbücken, Reports on Progress in Physics 47 (1984) 399–459.

[40] J. A. Giacomo, A Low Energy Electron Microscopy study of the growth and surface dynamics of Ag/Ge(111) and Au/Ge(111), Ph.D. thesis, University of California, Davis, 2009.

[41] P. Meakin, Reports on Progress in Physics 55 (1992) 157–240.

[42] F. A. Nichols, Journal of Nuclear Materials 30 (1969) 143–165.

[43] W. W. Mullins, G. S. Rohrer, J. Am. Ceram. Soc. 83 (1) (2000) 214–216.

[44] T. Radetic, E. Johnson, D. L. Olmsted, Y. Yang, B. B. Laird, M. Asta, U. Dahmen, Acta Materiala 141 (2017) 427–433.

[45] B. H. Stenger, A. L. Dorsett, J. H. Miller, E. M. Russell, C. A. Gabris, S. Chiang, Ultramicroscopy 183 (2017) 72–76.

[46] W. Yang, H. Ade, R. Nemanich, Phys. Rev. B 69 (4).

[47] T. Ichinokawa, H. Izumi, C. Haginoya, H. Itoh, Phys. Rev. B 47 (15) (1993) 9654–9657.

[48] P. Bampoulis, L. Zhang, A. Safaei, R. van Gastel, B. Poelsema, H. J. W. Zandvliet, Journal of Physics-Condensed Matter 26 (44).